

AD-A091 298

ARMY ARMAMENT RESEARCH AND DEVELOPMENT COMMAND ABERD--ETC F/6 7/4
COLLISION-INDUCED TRANSFER RATES CONNECTING FINE-STRUCTURE LEVE--ETC(U)
AUG 80 T A CAUGHNEY, D R CROSLLEY

UNCLASSIFIED

ARBRL-TR-02259

SBIE-AD-E430 518

NL

1 of 1
AD-A
091241



END
DATE
FILMED
12-80
DTIC

LEVEL III (12)
H

AD-E430518

AD A091248

AD

TECHNICAL REPORT ARBRL-TR-02259

COLLISION-INDUCED TRANSFER RATES
CONNECTING FINE-STRUCTURE LEVELS IN

$$S_2(B^3\Sigma_u^-, v' = 4)$$

Thomas A. Caughey
David R. Crosley

August 1980

DTIC
ELECTE
NOV 5 1980
S B



US ARMY ARMAMENT RESEARCH AND DEVELOPMENT COMMAND
BALLISTIC RESEARCH LABORATORY
ABERDEEN PROVING GROUND, MARYLAND

Approved for public release; distribution unlimited.

DDC FILE COPY

80 10 16 101

Destroy this report when it is no longer needed.
Do not return it to the originator.

Secondary distribution of this report by originating
or sponsoring activity is prohibited.

Additional copies of this report may be obtained
from the National Technical Information Service,
U.S. Department of Commerce, Springfield, Virginia
22151.

The findings in this report are not to be construed as
an official Department of the Army position, unless
so designated by other authorized documents.

*The use of trade names or manufacturers' names in this report
does not constitute endorsement of any commercial product.*

UNCLASSIFIED

SECURITY CLASSIFICATION OF THIS PAGE (When Data Entered)

REPORT DOCUMENTATION PAGE		READ INSTRUCTIONS BEFORE COMPLETING FORM
1. REPORT NUMBER	2. GOVT ACCESSION NO.	3. RECIPIENT'S CATALOG NUMBER
TECHNICAL REPORT ARBRL-TR-02259	AD-A091248	
4. TITLE (and Subtitle)	5. TYPE OF REPORT & PERIOD COVERED	
COLLISION-INDUCED TRANSFER RATES CONNECTING FINE-STRUCTURE LEVELS IN $S_2(B^3\Sigma_u^-, v' = 4)$	BRL TECHNICAL REPORT	
7. AUTHOR(s)	6. PERFORMING ORG. REPORT NUMBER	
Thomas A. Caughey* David R. Crosley**		
9. PERFORMING ORGANIZATION NAME AND ADDRESS	8. CONTRACT OR GRANT NUMBER(s)	
U.S. Army Armament Research and Development Command U.S. Army Ballistic Research Laboratory ATTN: DRDAR-BLP Aberdeen Proving Ground, MD 21005		
11. CONTROLLING OFFICE NAME AND ADDRESS	10. PROGRAM ELEMENT, PROJECT, TASK AREA & WORK UNIT NUMBERS	
U.S. Army Armament Research and Development Command U.S. Army Ballistic Research Laboratory ATTN: DRDAR-BL Aberdeen Proving Ground, MD 21005		
14. MONITORING AGENCY NAME & ADDRESS (if different from Controlling Office)	12. REPORT DATE	
	Aug 1980	
	13. NUMBER OF PAGES	
	34	
	15. SECURITY CLASS. (of this report)	
	Unclassified	
	15a. DECLASSIFICATION/DOWNGRADING SCHEDULE	
16. DISTRIBUTION STATEMENT (of this Report)		
Approved for public release; distribution unlimited		
17. DISTRIBUTION STATEMENT (of the abstract entered in Block 20, if different from Report)		
18. SUPPLEMENTARY NOTES		
* Present address: Interactive Radiation, Inc., Northvale, NJ 07647		
** Present address: Molecular Physics Laboratory, SRI International, Menlo Park, CA 94025		
19. KEY WORDS (Continue on reverse side if necessary and identify by block number)		
Energy Transfer Rotational Relaxation S_2 Molecule State-to-State Transfer		
20. ABSTRACT (Continue on reverse side if necessary and identify by block number)		
(c1t) Rates for collision-induced transfer between a single rotational level ($v = 4, J = 41$) and other individual rotational levels within the same vibrational level of the B-state of diatomic sulfur are reported. The sulfur was excited into the B-state by the radiation from an atomic zinc lamp, and rotationally resolved fluorescence measurements were used to determine the rates for the collision partners He, Ar and Xe.		

TABLE OF CONTENTS

	<u>Page</u>
I. INTRODUCTION	5
II. TRANSITIONS FREQUENCIES AND ASSIGNMENTS	6
III. EXCITED STATE POPULATIONS	10
IV. RATE CONSTANTS	14
V. DISCUSSION	19
ACKNOWLEDGMENTS	23
REFERENCES	26
APPENDIX	27
DISTRIBUTION LIST	29

Accession For	
NTIS GRA&I	<input checked="" type="checkbox"/>
DTIC TAB	<input type="checkbox"/>
Unannounced	<input type="checkbox"/>
Justification	
By _____	
Distribution/	
Availability Codes	
Dist	Avail and/or Special
A	

I. INTRODUCTION

Collisional energy transfer between individual quantum states of simple molecules has been the subject of much recent experimental endeavour, in an attempt to better understand detailed collision dynamics. We report here rates for energy transfer into a number of different rotational and fine-structure levels, starting from a single initially excited level, within a particular vibrational level of the $B^3\Sigma_u^-$ electronically excited state of diatomic sulfur. The S_2 is excited by absorption of line radiation from a lamp containing Zn; rotationally resolved fluorescence measurements at various pressures of the collision partners He, Ar and Xe permit extraction of the rates.

The experiments described here are similar to our earlier measurements at lower resolution,¹ in which we determined vibrational and total rotational transfer rates from this same initially excited level ($v'=4$, $N'=40$, $J'=41$). The sums of the state-to-state rates found here are compatible with the total rotational rates reported in I. The state-to-state rates are also compatible with, and have been used to analyze data in, a study of the degree of coherence retention in rotationally inelastic collisions within this level.² These three aspects all form component pieces of the overall collision dynamics of electronically excited S_2 . The B-state is a very suitable molecule for a comprehensive mapping of its collisional behavior, particularly due to the ease of fluorescence excitation in a wavelength region convenient to frequency-doubled, tunable lasers.

The basic experimental apparatus has been described in I. Briefly, a cell containing S_2 at ~ 150 mtorr pressure and 900 K is irradiated with the light from a Zn/Ar flow lamp powered by a 2450 MHz discharge. As in I, lamp stability proved quite important; the present measurements are at higher resolution and thus at a lower signal level than those described in I, and again require long, drift-free scans. The fluorescence at right angles to the exciting radiation was focused into a 3/4-m Spex monochromator, operated in second order. With entrance/exit slit widths of 30/60 μ and 10mm slit height, an instrumentally determined trapezoidal line shape with a full-width at half-maximum (first-order equivalent) of 0.4 \AA was obtained. Fluorescence spectra of the $v'=4$, $v''=2$ band were recorded at a series of foreign gas pressures at a scan rate of 0.5 $\text{\AA}/\text{min}$. The lamp intensity was continually monitored by a second monochromator, in order to correct for small drift.

¹T. A. Caughey and D. R. Crosley, "Collision-Induced Energy Transfer in the $B^3\Sigma_u^-$ State of Diatomic Sulfur", *J. Chem. Phys.*, **69**, 3379-3396 (1978), referred to as I.

²T. A. Caughey and D. R. Crosley, "Coherence Retention During Rotationally Inelastic Collisions of Selectively Excited Diatomic Sulfur", *Chem. Phys.* **20**, 467-476, (1977).

Figure 1 shows the development of the spectrum as the He pressure is increased. A cursory examination reveals the importance of single collision, multiquantum transfer ($\Delta N > 2$). First, the highest pressure illustrated corresponds to only about 15 percent of the S_2 having undergone any transfer collisions, yet many levels are clearly populated. Further, the intensities of lines corresponding to multiquantum transfer grow, with increasing pressure, in direct linear proportion to that of lines corresponding to transfer to adjacent levels, and not in geometric proportion. At higher pressure, the effects of multiple collisions become readily apparent. Since we desire to obtain relative final-state cross sections for single collisions, it is necessary to restrict the measurements to the relatively low pressures displayed in Figure 1. Thus we can obtain reliable values for transfer rates (that is for rates, ~ 20 percent of the largest single-collision rate) only for final-J values in the vicinity of the initially pumped level.

In turn, this means that most of the pertinent data comes from lines in the neighborhood of those emitted by the initially excited level. A number of these lines are closely packed, and sometimes overlapped, with the resolution which we employ. In several early experiments using sulfur of natural abundance, it was found that emission from levels of ^{34}S - ^{32}S , directly excited by absorption of various Zn lines, greatly hampered the intensity measurements of the weak emission from transferred ^{32}S - ^{32}S molecules. Consequently all of the experiments reported here were carried out on samples of sulfur enriched in ^{32}S abundance.

The closely spaced rotational lines of the ^{32}S - ^{32}S isotope make it necessary to calculate their transition frequencies within the (heretofore unanalyzed) $v' = 4$, $v'' = 2$ band in order to obtain unambiguous assignments. In the following we describe this procedure, the determination of level populations from the measured intensities, and the extraction from these pressure-dependent populations of several final-state-specific transfer rates.

II. TRANSITIONS FREQUENCIES AND ASSIGNMENTS

Consider first the appearance of the spectrum when only a single level is emitting. Because ^{32}S - ^{32}S is a homonuclear diatomic and ^{32}S has zero nuclear spin, alternate rotational levels are missing in each state. In the ground $X \ ^3\Sigma_g^-$ state, only odd-numbered rotational levels exist, whereas in the $B \ ^3\Sigma_u^-$ state, only even rotational levels are allowed. Coupling the unit electron spin with a rotational angular momentum produces three distinct levels characterized by the value of the resultant total angular momentum J and separately denoted as either an F_1 ($J=N+1$), an F_2 ($J=N$), or an F_3 ($J=N-1$) level. In such a picture of pure Hund's case-b coupling, only two rotational branches are allowed in emission from a single N' , J' level. Deviation from pure case-b coupling leads to the appearance of two additional rotational branches when the fluorescing state is either an F_1 or an F_3 level. As has been discussed

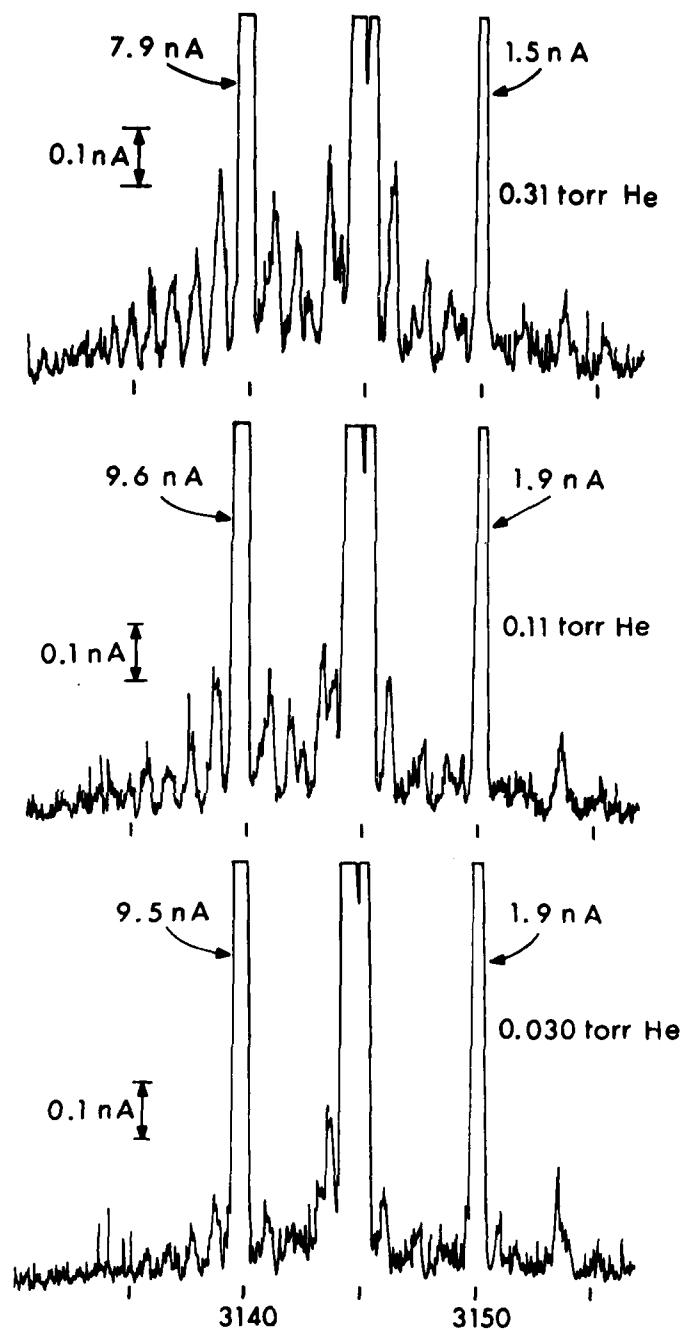


Fig. 1. The development of rotational relaxation in S_2 upon increasing the pressure of helium fill gas. A scan of the (4,2) band is shown, in which appear a number of lines due to rotationally transferred molecules. The four lines emitted by the initially pumped F_1 (40) level are off scale in the figure; the peak photocurrent of the R_1 and N_{P13} branches are given in each case next to these two lines for comparison with the transferred fluorescence.

for the present transition,³ emission from the $v'=4$, $N'=40$, $J'=41$ level of ^{32}S - ^{32}S consists of four rotational branches. Two of these have⁴ $\Delta J=\Delta N$, and are relatively intense: the R_1 line with $\Delta J=\Delta N=+1$ and the P_1 line with $\Delta J=\Delta N=-1$. In addition there exist two weaker lines, each with about one-fifth the intensity of the R_1 and P_1 branches. These are the $^{PR}_{13}$ line ($\Delta J=+1$, $\Delta N=-1$) and the $^{NP}_{13}$ line ($\Delta J=-1$, $\Delta N=-3$). Despite the deviation from case-b coupling, each level is still referred to by its F_i designation. We shall specify a level by calling it the F_i (N') level, e.g. the initially pumped level is F_1 (40) since $N'=40$ and $J'=41$.

In Figure 1, the four lines emitted by F_1 (40) are all off-scale at the sensitivity employed. They are marked in the uppermost scan, and in each case the intensities of the R_1 and $^{NP}_{13}$ branches at the gain setting are noted for comparison with the magnitude of the weak transferred features.

It was necessary to carry out scans at zero pressure of added gas, since even with the enriched-isotope sample there remain a number of definite, reproducible peaks (of intensity 1 to 2 percent of the R_1 line) in the (4,2) band region. These are perhaps due to 'secondary' weaker fluorescence series excited in ^{32}S - ^{32}S by other Zn lines, to scatter from lamp impurities, or to some small amount of rotational relaxation caused by residual foreign gases in the cell. In any case, a baseline correction, scaled to the intensity of the rotational branches of F_1 (40), was calculated for each feature from zero pressure scans and was subtracted from the baselines of transferred spectra.

As mentioned above, it was necessary to calculate transition frequencies within the (4,2) band in order to obtain line assignments. For this, Naude's analysis⁵ of the (4,19) band was used, along with a calculation of the energy separation between the ground state $v''=2$ and $v''=19$ levels based on a set of ground state spectroscopic constants given by Barrow⁶. The accuracy of using these ground state constants was checked by comparing calculated energy separations between rotational levels of

³K. A. Meyer and D. R. Crosley, "Rotational Satellite Intensities and Triplet Splitting in the $B^3\Sigma_u^-$ state of S_2 ", *Can. J. Phys.* 51, 2119-2121, (1973).

⁴As is customary, $\Delta J \equiv J' - J''$ and $\Delta N \equiv N' - N''$ here.

⁵S. M. Naude, "Die Rotationsstruktur des Bandenspektrums des Schwefelmoleküls S_2 ", *Ann. Phys. (Leipz)* 3, 201-222, (1948).

⁶R. F. Barrow and R. P. du Parcq, in *Elemental Sulfur*, edited by B. Meyer (Interscience, New York, 1965), p. 251.

$v''=2$ and $v''=19$ with the separations derived from the rotationally analyzed (3,2)⁵ and (3,10)⁷ bands. The calculated ground state separations were found to be uniformly too small by 1.34cm^{-1} when compared to the direct experimental data, with random variations about this mean of up to 0.2cm^{-1} . Since the identification of fluorescence from transferred levels is based on its wavelength shift from the main fluorescence lines, a systematic uncertainty in the calculation is of no importance and we obtain internally precise results.

The uncertainty in the transition frequencies for each of the rotationally analyzed bands is given as only several hundredths of a wavenumber, so that our calculated values should be within at least 0.3cm^{-1} of the exact frequencies. In the wavelength region of the (4,2) band, there are approximately 10cm^{-1} per Å so that a 0.3cm^{-1} or 0.03 Å uncertainty in the relative position of a line is insignificant compared to an instrumental linewidth of 0.4 Å. The levels, whose energies are directly available from the literature, extend to large N' values inclusive of F_1 (54), F_2 (44), and F_3 (36). To find the energies of higher lying levels, a short extrapolation to larger N' was made by plotting second differences vs. N' . For the F_3 (48) level, for which the longest extrapolation was required, we expect an uncertainty of no more than 1cm^{-1} , or 0.1 Å, due to accumulated uncertainty in determining the successive levels above F_3 (36). Thus, all directly available and extrapolated transition frequencies should accurately pinpoint the positions of rotational lines, barring any substantial perturbations which would invalidate the extrapolated values.

When making the extrapolation to higher N' for the F_2 manifold, we noted a deviation⁷ from the expected smooth variation of second differences N' . Since ground state rotational levels were already verified to change smoothly with N'' , the variation must be in the excited state. It appears that the F_2 levels are perturbed in the neighborhood of $N'=38$ and $N'=40$ and possibly near $N'=44$. The presence of this perturbation may affect the fine details of the collisional rotational relaxation. Specifically, it may influence the relative size of relaxation to F_2 and F_3 levels. Aside from affecting the actual dynamics of the process, intensities of the perturbed levels may be markedly different than in the unperturbed case, making the apparent size of collisional relaxation to these states, based on fluorescence intensity, incorrect. It is true, however, that the F_2 (42) level appears to be unperturbed, and it is the single-collision transfer rate to the F_2 (42) level which we report.

The above consideration is also a reminder that, in studying transfer from only one level as is done here, the generality of results obtained can be open to question since the single level investigated may behave anomalously. In the present case, the smooth variation of second difference for F_1 levels in the vicinity of $N'=40$ confirms that our initial F_1 (40) level is indeed unperturbed.

⁷E. Olsson, "Das Bandenspektrum des Schwefels", *Z. Phys.* 100, 656-664 (1936).

Figure 2 exhibits a scan of the (4,2) band in the presence of $\sim 1/3$ torr Ar. The positions of a number of lines predicted by the above method are indicated on the figure. It should be noted that these assignments are not fitted to the spectrum shown, but rather the calculated and measured positions are separate absolute wavelengths. (The largest uncertainty in an individual scan comes from non-linearities in the spectrometer-monochromator plus recorder-wavelength recording. Repetitive scans of the region, however, remove any assignment uncertainties.) From the correspondence of predicted positions with observed peaks and shoulders, as exemplified in Fig. 2, we conclude that we have attained an unambiguous assignment of the major transfer features appearing under single-collision conditions.

III. EXCITED STATE POPULATIONS

Several fortuitous circumstances enable us to observe some rotational structure in a molecule as heavy as S₂. For one, the energy ordering at these values of N in the excited state is $F_1 > F_3 > F_2$ which is exactly reversed from the energy ordering in the ground state at these N, where $F_2 > F_3 > F_1$. Hence, fluorescence from the different F_i levels of a given N' is more easily resolved than if the relative ordering of the levels were the same in both states. Secondly, as already mentioned, alternate rotational levels are missing in both the ground and excited states. Thirdly, the zinc excitation occurs at a relatively high N--out in the tail of the band where the rotational spacing becomes spread out.

In the wavelength region between the P_{R13} and N_{P13} lines, shown in Fig. 2, close agreement is found between calculated positions and resolved features. Close agreement also is found in the shorter wavelength region, below about 313.8 nm. However, the higher density of lines and frequent overlapping in this region make an unambiguous analysis of intensities of those individual lines very difficult. For this reason, we did not measure any rates to levels of N' less than 40 for F_2 or F_3 levels nor rates to levels of N' less than 34 for F_1 levels. Instead, more dependence was placed on the region between the P_{R13} and N_{P13} lines where the effective resolution of the rotational structure is greater.

Following the application of the zero-pressure baseline correction, the intensity of the rotationally resolved features is measured. The intensity of an emission line from a transferred level is taken as proportional to the population of that level, and the intensity of the P_1 branch of F_1 (40) is taken as a measure of the F_1 (40) state population. The ratio of a transferred population to the initial state population, as required for the steady-state analysis described in the following section, is then conveniently given by the ratio of the heights of the corresponding lines. All rotational line strengths are assumed equal for a given branch (e.g., the R_1 sequence). This introduces negligible

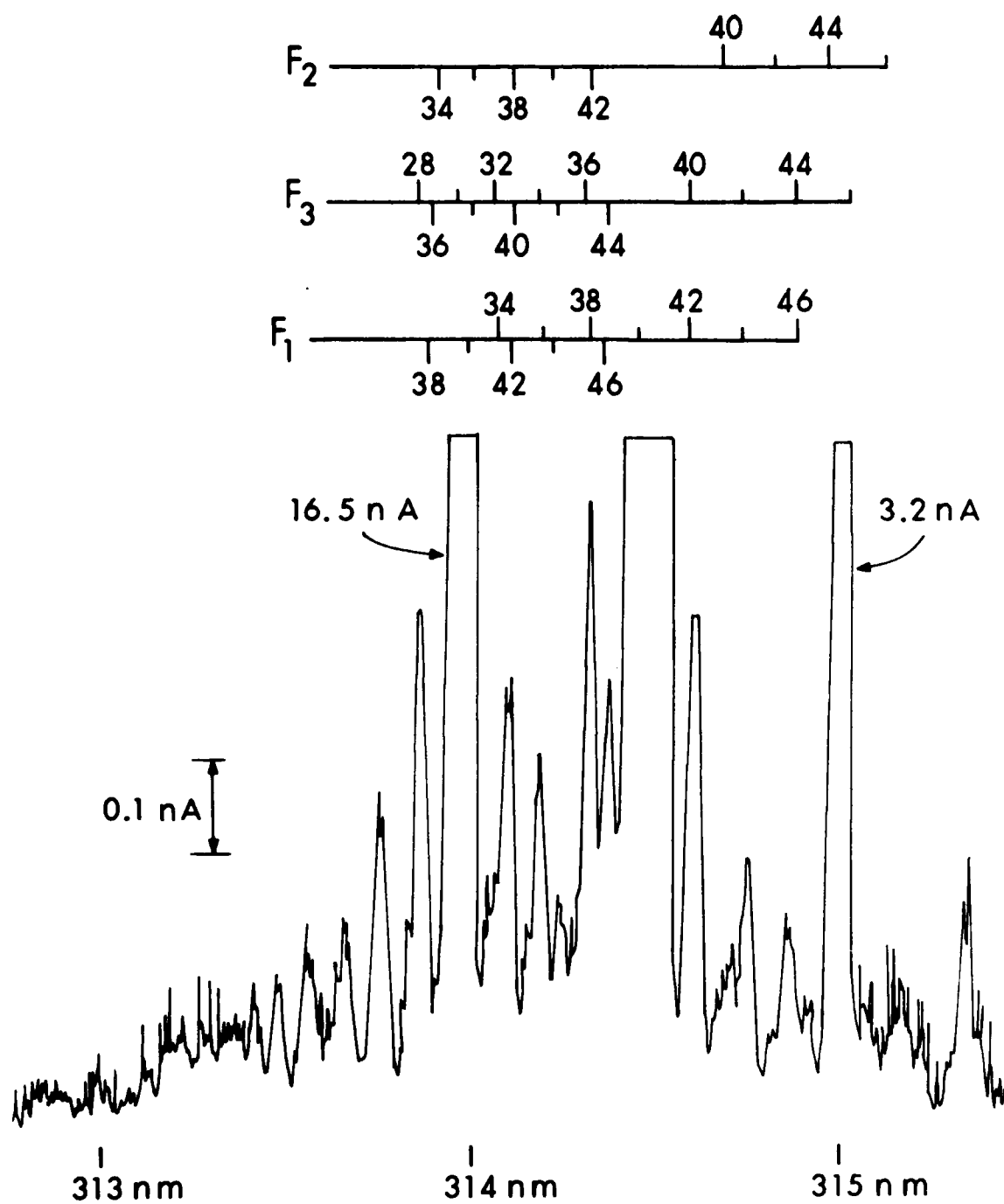


Fig. 2. A scan of the (4,2) band in the presence of 0.34 torr argon. As in Fig. 1, the peak photocurrents of the R_1 and Np_{13} branches are marked next to the top of those lines. The levels marked in the diagram are those responsible for emission lines at the particular wavelengths marked.

error; for example in case-b coupling the difference in relative line strengths of R_1 (34) and R_1 (48) is only 0.4 per cent. A given branch (R_2 or P_2) emitted by an F_2 level is 17 per cent more intense than the corresponding main branch emitted by F_1 or F_3 , due to the lack of satellite lines from F_2 , and this value is used in the analysis.

Even in the relatively well-resolved region between the P_{R13} and N_{P13} branches of F_1 (40), there still exists noticeable overlap of some lines, as is evident from Fig. 2. This overlap was accounted for using the experimentally determined bandpass, the calculated line positions, and manual iteration involving certain assumptions. As many populations as possible are first determined from isolated lines, and used to compute corrections necessary to subtract from blended features. When necessary for these iterations, estimates of F_3 populations for $N' \leq 36$ were obtained from the assumption of equal populations in the F_1 and F_3 levels. This is based on the close agreement of F_1 and F_3 populations for $N' \geq 44$, and the assumption of an up-down symmetry. (We found such an up-down symmetry for the F_1 levels, providing the motivation for assuming it to hold also for the F_3 levels). Also, due to the small intensity of F_2 (40) and F_2 (42) lines, contributions of F_2 levels to intensities in the R branch of F_1 levels were taken to be zero. Satellite intensities for F_1 and F_3 levels were taken to one sixth of the R or P intensity. Further numerical details concerning the analysis may be found in reference 8.

As an example of the quality of the data, Table I lists relative populations obtained in the runs with He as the collision partner. For nearly all levels, there exist two values of the population determined independently from the appropriate R_i and P_i branches. Approximate agreement of populations determined from the R and P branches of F_1 levels is noteworthy since height corrections to the R branch involved mostly F_2 and F_3 levels with $N' < 40$, whereas height corrections to the P branch involved populations of F_2 and F_3 levels with $N' > 40$ and were free of the above-mentioned assumptions about the F_2 and F_3 level populations.

Uncertainties in intensity measurements introduce about ± 0.4 in the population ratios of Table I. A range of values is quoted for a few populations due to uncertainty in deciding how much intensity is attributable to a level in a crowded region of spectrum.

Table I exhibits not only the agreement between R and P branch determined populations, but also the reproducibility between two successive scans across the (4,2) band with the 0.31 torr fill gas pressure of helium. The disparity between the R and P branch data for $F_1(44)$ at 0.31 torr is reproducible here, but such a disparity was not apparent with the other two gases so that its probable cause is not evident to us.

⁸T. A. Caughey, "Collisional Energy Transfer in B-State Diatomic Sulfur", Ph. D. Thesis, University of Wisconsin, Madison, WI, (1977).

TABLE 1
POPULATION RATIOS FOR He RUNS
NORMALIZED TO POPULATION OF F_1 (40) = 1000

N	0.03 torr			0.11 torr			0.31 torr, Run A			0.31 torr, Run B		
F ₁ levels	R	P		R	P		R	P		R	P	
50	-	1.3		-	3.0		-	6.8		-	5.6	
46	-	2.1		-	6.4		-	12.3		-	10.4	
44	2.5	3.2		7.2	6.3		9.0	18.9		7.9	16.7	
42	4.3	2.9		15.1	14.3		30.7	30.4		23.2	32.0	
40	-	1000.0		-	1000.0		-	1000.0		-	1000.0	
38	5.1	4.4		12.3	12.5		26.6	26.7		25.1	28.8	
36	3.7	1.2		6.7	6.4		14.7	15.5		13.2	17.4	
34	2.7	-		5.9	-		11.9	-		10.6	-	
F ₃ levels												
48	-	3.3		-	3.4		-	7.5		-	11.1	
44	-	2.2		-	6.4		-	14.3		-	11.1	
42	-	1.7		-	3.9		-	11.3		-	10.4	
40	-	0 to 4.2		-	3.3		-	9.8		-	4.2 to 7.7	
F ₂ levels												
42	-	0.5		-	-		-	1.3 to 2.5		-	-	

IV. RATE CONSTANTS

Prior to a consideration of the quantitative determination of the rate constants, we can make two qualitative observations from a rather direct examination of the raw data. First, the rotational transfer process is a multi-quantum affair, that is, the molecule is not limited in transfers only to adjacent levels. This can be seen from the scans of Fig. 1, which show the development of rotational transfer as helium pressure is increased. The lines to the short wavelength side of the R₁ line of F₁ (40) (while actually blends of several lines) are to a large extent at these low helium pressures the R₁ lines of F₁ (38), F₁ (36), F₁ (34), etc. Were the transfer process limited to downward transfers of only $\Delta N = -2$, for example, and if the transfer rates for the F₁ (N') levels were reasonably independent of N', then one would expect a geometrical decrease in the intensities upon going to shorter wavelengths. For example, if F₁ (38) were 5 per cent of F₁ (40) as in the 0.03 torr He scan the F₁ (36) should be about 5 per cent as intense as F₁ (38),... However, since the intensities do not fall off this quickly, $\Delta N > 2$ processes must be quite probable. One safely can count out seven such peaks to shorter wavelengths, thereby showing that changes up to at least $\Delta N = 14$ do occur as a result of a single collision.

One also notes that the relative probability of transfer to F₁ vs. non-F₁ levels is different for some N', even though the triplet splitting here is smaller than the rotational spacing. For example, a comparison of intensities in the P-branch region of Fig. 2 shows that the F₁ (42) level has a larger population than either F₂ (42) or F₃ (42). Hence, size of the energy gap is not the only important factor for determining transfer probabilities.

The analysis of the pressure dependence of the populations, so as to extract rate constants for the energy transfer, is carried out using a steady state balance applied to S_J^{*}, the population of the Jth rotational level in the excited state. The development of the equations, closely paralleling that of Steinfeld⁹ for similar work in I₂, is treated in detail in I. The resulting working equation is

$$[1 + Q_S' S + (Q' + V' + R') A] (S_J^*/S_{41}^*) = R'_{41,J} A. \quad (1)$$

Here, A is the foreign gas pressure, S is the ground state S₂ pressure, S_J^{*} is the population of the Jth rotational level,¹⁰ and S₄₁^{*} is the

⁹J. I. Steinfeld and W. Klemperer, "Energy Transfer in Monochromatically Excited Iodine Molecules", *J. Chem. Phys.* **42**, 3475 (1965).

¹⁰More precisely, the N, J level since both quantum numbers are actually necessary for a full description.

population of the $J=41$ pumped level. The rate constant $R'_{41,J}$ is for transfer from F_1 (40) to the J^{th} level. Q' , V' and R' are rate constants for quenching, vibrational transfer, and total rotational transfer from the J^{th} level. Q_S' is the rate constant for quenching due to collisions with ground state S_2 ; vibrational and rotational transfer in S_2 (B)- S_2 (X) collisions is negligible.^{1,2} The rate constants are conveniently measured in units of a per number density per radiative lifetime (τ) basis, and the primes denote multiplication by τ .

Values for the parameters on the left-hand side of Eq (1) are taken from I. There, values of Q_S' , Q' , V' , and R' were measured for transfer out of the initially pumped F_1 (40) level. For analysis of the current data, it is necessary to assume that none of these parameters, nor τ , vary with rotational level, so that the results for F_1 (40) may be considered to describe the behavior of the level denoted by J . While the lifetime appears shorter¹¹ for a low rotational level ($J'=13$) in $v'=4$, these parameters probably do not vary much over the range of J (34-50) probed here. A value for $\tau = 36$ nsec¹¹ is used to reduce the values of $R'_{41,J}$ to absolute units; the relationship between number density and measured pressure, also needed, is discussed in detail in I.

Thus when the left-hand side of Eq (1), containing the measured ratio S_J^*/S_{41}^* and previously determined values, is plotted vs. A , a straight line should result. The slope then yields the value of $R'_{41,J}$. A few exemplary plots for He are shown in Fig. 3. The slopes for each of the three gases are then used to obtain the transfer rates, which are presented in Tables 2 and 3 in the form of rate constants ($\text{cm}^3 \text{ sec}^{-1}$) and cross sections¹² (\AA^2), respectively.

Pressures have been kept low here in order to minimize multiple collisions of the excited molecule. Using the values of R' obtained in I, we find that at the highest pressures used, about 15 per cent of the excited molecules have undergone a single rotational-state-changing collision, while 3.4 per cent have undergone two or more such collisions (see Appendix). Vibrational back transfer (a necessary consideration in the analysis for total rotational transfer in I) need not be considered here since the adjacent vibrational levels are so sparsely populated at the pressures used in these experiments. Hence, we remain in a pressure regime low enough such that Eq (1) can be meaningfully applied, yet high enough to obtain results with a presentable level of precision.

The errors bars on the final results come from two sources. The first is the obvious uncertainties in the measured population ratios,

¹¹T. A. Caughey, K. A. Meyer and D. R. Crosley, "Lifetimes in the $B^3\Sigma_u^-$ State of S_2 ", to be published.

¹²The cell temperature of 900 K is used to calculate the mean relative velocity.

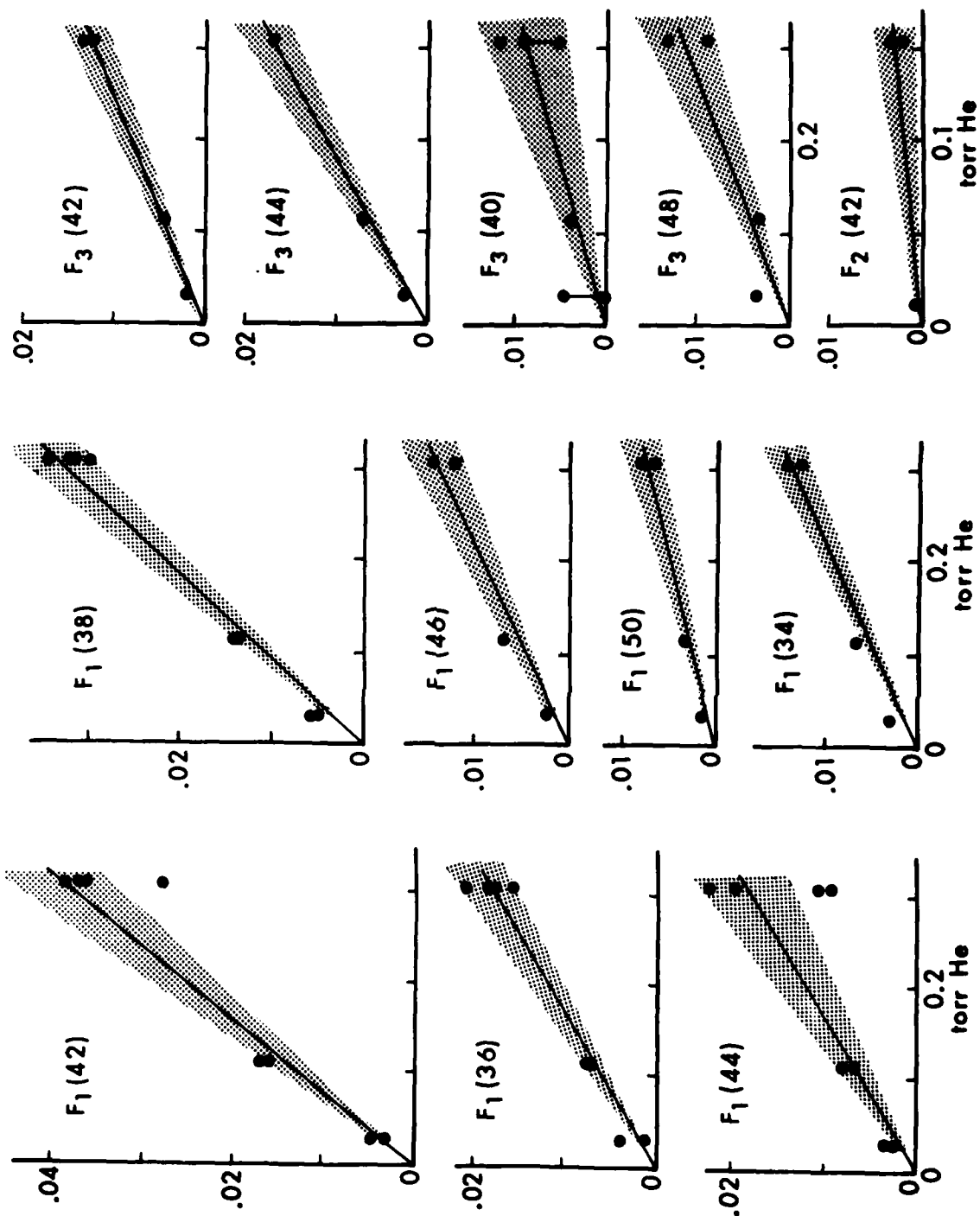


Fig. 3. Plots of the quantity given on the left-hand-side of Eq. (1), for a number of different final states, versus pressure of He. The straight lines drawn are the fits to the data points used to obtain the quoted results, and shaded area denotes the fit limits corresponding to the quoted error bars.

TABLE 2. STATE-to-STATE ROTATIONAL RELAXATION RATES
(units = 10^{-10} cm³/sec·molecule)

	He	Ar	Xe
F_1 levels			
50	0.24±0.07	0.17±.08	0.13±0.03
46	0.45±0.09	0.26±.09	0.16±0.03
44	0.58±0.15	0.32±.11	0.18±0.05
42	1.21±0.18	0.80±.14	0.39±0.07
38	1.05±0.12	0.71±.15	0.42±0.08
36	0.57±0.09	0.33±.08	0.19±0.05
34	0.43±0.07	0.24±.06	0.18±0.03
F_3 levels			
48	0.36±0.11	0.14±.07	0.10±0.03
44	0.54±0.09	0.29±.08	0.09±0.03
42	0.40±0.08	0.27±.09	0.07±0.03
40	0.27±0.15	0.18±.09	0.07±0.03
F_2 level			
42	0.07±0.06	0.06±0.06	0.08±0.08
40	-	-	0.04±0.04

TABLE 3. STATE-to-STATE ROTATIONAL TRANSFER CROSS-SECTIONS (\AA^2)

	He	Ar	Xe
F_1 levels			
50	1.1 ± 0.3	1.9 ± 0.9	1.9 ± 0.5
46	2.0 ± 0.4	3.0 ± 1.1	2.4 ± 0.5
44	2.6 ± 0.7	3.7 ± 1.3	2.7 ± 0.8
42	5.4 ± 0.8	9.0 ± 1.6	5.8 ± 1.0
38	4.7 ± 0.5	8.0 ± 1.8	6.3 ± 1.2
36	2.5 ± 0.4	3.8 ± 0.9	2.9 ± 0.8
34	1.9 ± 0.3	2.7 ± 0.7	2.7 ± 0.4
F_3 levels			
48	1.6 ± 0.5	1.6 ± 0.8	1.5 ± 0.5
44	2.4 ± 0.4	3.3 ± 0.9	1.3 ± 0.5
42	1.8 ± 0.3	3.1 ± 1.0	1.1 ± 0.5
40	1.2 ± 0.7	2.0 ± 1.0	1.0 ± 0.5
F_2 levels			
42	0.33 ± 0.25	0.7 ± 0.7	1.1 ± 1.1
40	-	-	0.6 ± 0.6

which forms the largest contribution. Uncertainties in V' and R' contribute about 2.5 per cent uncertainty to the final values of $R'_{41,J}$. The error bars quoted in Tables 2 and 3 are maximum values, that is, they consider all errors as additive and are taken from slopes which include nearly all of the data points (see the shaded areas in Fig. 3).

V. DISCUSSION

The cross sections of Table 3 are plotted in Fig. 4 vs. the final rotational quantum number for each of the collision partners studied. Although there is some overlap of error bars (see Table 3), we can nonetheless make some definite statements about trends in the cross sections: (i) single-collision cross sections for transfer to F_1 levels decrease with increasing value of $|\Delta N|$; (ii) a range of rotational levels may be populated after a single collision; (iii) for the range of $|\Delta N|$ studied here there is a definite up-down symmetry to the data, that is, $\sigma(\Delta N) \sim \sigma(-\Delta N)$ for the F_1 levels; (iv) for small ΔN , there is a preference for transfer to other F_1 levels over transfer to the F_3 or the F_2 level of the same N' and (v) the maximum rate for transfer to an F_3 level does not occur for $N'=42$.

A more quantitative, though empirical, treatment of points (i), (ii), and (iii) can be obtained using the techniques of surprisal analysis. The question is whether the trends in the F_1 cross sections with ΔN simply reflect increases in the energy defect with increasing $|\Delta N|$, or whether an additional dynamical variation with ΔN exists. In this context, it is useful to note that the largest energy difference for which we have measured a cross section, viz., $E(50)-E(40)$, is less than $1/3$ of kT .

Prior rate constants $k_p(N_f)$ were calculated according to the equation pertinent to rotational energy transfer caused by a structureless particle:¹³

$$k_p(N_f) = c g_f \delta \exp(\pm \delta/2) K_1(\delta/2) \quad (2)$$

where c is a constant, g_f is the final-state degeneracy, $\delta = |E_f - E_i|/kT$, and K_1 is the first-order modified Bessel function of the second kind. The plus sign in the exponential is used if $E_f < E_i$ and the minus sign when $E_f > E_i$. The surprisal, defined by

$$I(N_f) = -\ln [k(N_f) / k_p(N_f)], \quad (3)$$

¹³M. Robinson and J. I. Steinfeld, "Entropy Analysis of Product Energy Distributions in Nonreactive Inelastic Collisions", *Chem. Phys.* **4**, 467-475 (1974).

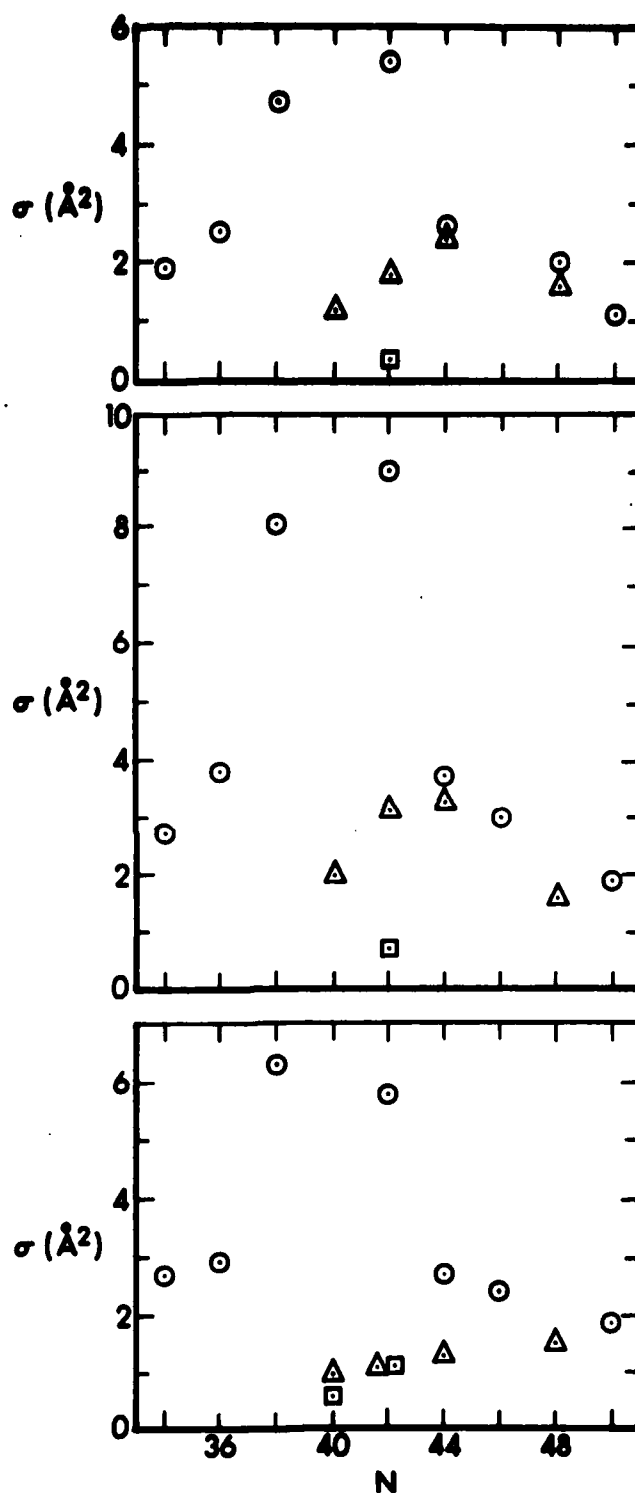


Fig. 4. Plots of the individual cross sections of Table 3 vs. final-state rotational quantum number. Circles are for transfer to F1 levels, triangles for F3 levels, and squares for F2 levels. Top: Helium; Middle: Argon; Bottom: Xenon.

is often found to behave linearly on energy difference

$$I(N_f) = \text{const} + \lambda \delta. \quad (4)$$

The slope is often called the surprisal parameter, and, if I obeys the functional relationship of Eq. (4), is a convenient measure of the nature of the energy transfer collisions.

Surprisal plots for the F_1 level transfer, for each of the three gases, are given in Fig. 5. All of the multiquantum transfer ($\Delta N > 2$) points fall on a straight line for each gas (that is, each gas differs in the value both of the constant and of λ in Eq. (4)). Values of λ taken from these curves are: He, $\lambda = 4.6$; Ar, $\lambda = 3.4$; Xe, $\lambda = 1.92$. The points for transfer to adjacent levels fall uniformly above the curves and are not included in the fits, perhaps suggesting a somewhat different mechanism also operative for collisions to adjacent rotational levels.

Values of λ much larger than one imply that the collisions tend toward the adiabatic limit, that is, a relatively brief collision in which the final outcome is not statistical but reflects a dynamic bias or propensity toward certain final states. It was argued in I that a physical picture of the trends in total vibrational and rotational relaxation rates with increasing mass of the collision partner tended toward a brief collision. In addition, a surprisal parameter of 1.3 described well the model multiquantum rate constants which in turn fitted the vibrational population evolution with increasing pressure. We conclude that the final-state-specific rates found here are again in accord with such an overall picture of the collisional behavior of $B^3\Sigma_u^- S_2$.

A definite indication of dynamic bias is also contained in the findings that $\sigma(F_1 \rightarrow F_3)$ and $\sigma(F_1 \rightarrow F_2)$ are generally smaller than $\sigma(F_1 \rightarrow F_1)$ for the same $|\Delta N|$. A propensity toward maintenance of the spin-rotation coupling during collisions has been found previously in the excited 2Σ states of NO¹⁴ and OH¹⁵. A simple physical picture suggests that the collision exerts torque on the rotational angular momentum \vec{N} , briefly decoupling it from the spin \vec{S} , whose orientation in space is unaffected. Recoupling of \vec{N} , and \vec{S} after the collision preserves their general orientation. This view is also appealing in the context of our findings, based on the retention of phase coherence following a rotationally inelastic collision,² that the orientation of the \vec{N} -vector is preserved in space even when its magnitude is changed by collision.

¹⁴H. P. Broida and T. Carrington, "Rotational, Vibrational and Electronic Energy Transfer in the Fluorescence of Nitric Oxide", *J. Chem. Phys.* **38**, 136-147 (1961).

¹⁵R. K. Lengel and D. R. Crosley, "Energy Transfer in $A^2\Sigma^+$ OH. I. Rotational", *J. Chem. Phys.* **67**, 2085-2101 (1977).

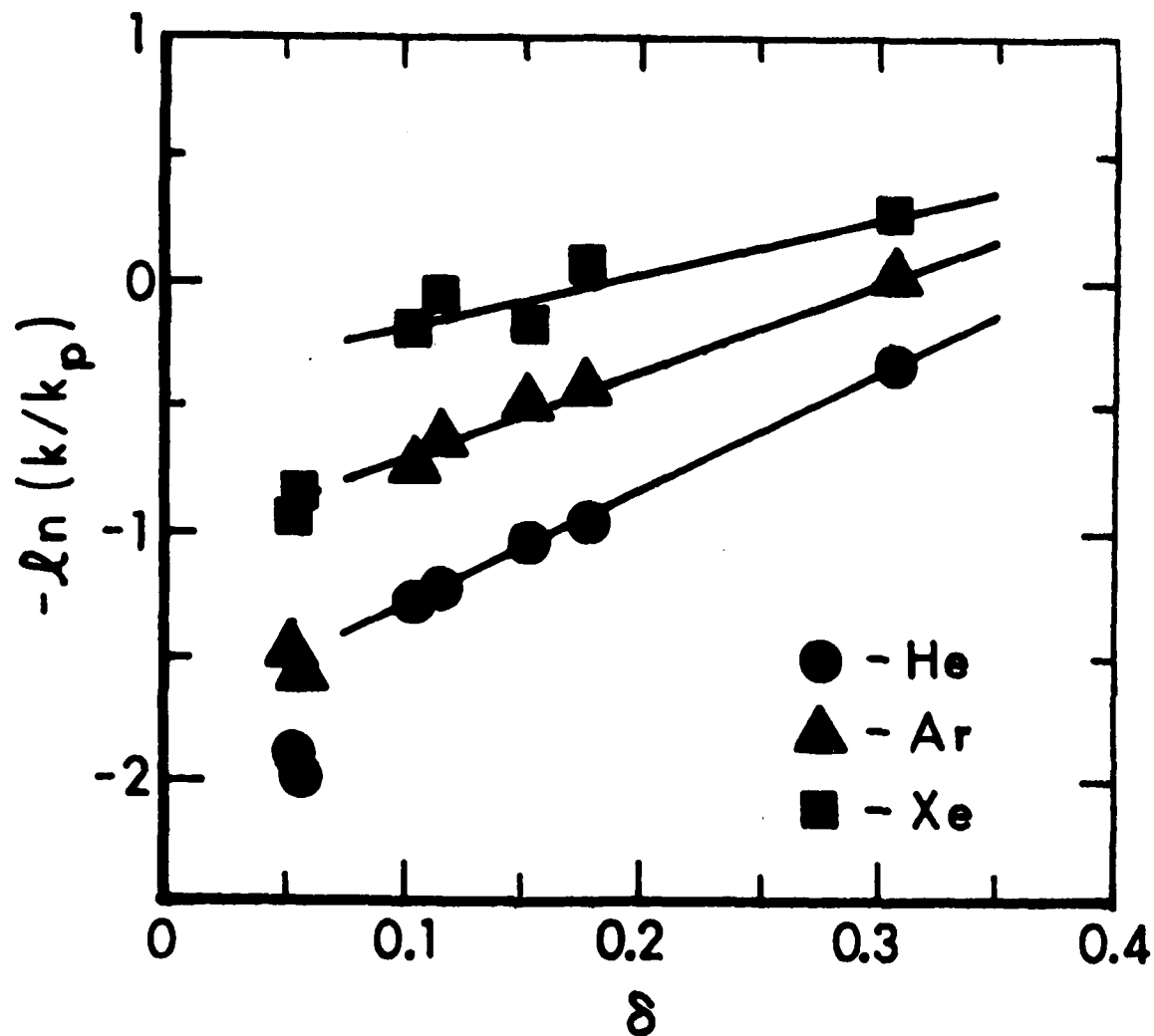


Fig. 5. Plot of the surprisal for the rate constants for transfer to F_1 levels. The abscissa δ is the absolute magnitude of the amount of energy transferred in the collision, divided by kT , so that upward and downward collisions are included. The straight lines correspond to the surprisal parameters quoted in the text; the lowest-energy transfer is not included in the fits. Circles: Helium; Triangles: Argon; Squares: Xenon.

The small size of the F_2 (42) cross-section should not be generalized to mean that little transfer occurs to all F_2 levels. In fact, the presence of F_2 transferred levels is quite noticeable. The accumulation of intensity near 3135.5 Å in Fig. 2, for example, occurs at the position of the F_2 band head. Hence, it is possible that the collisional preference for F_1 levels over F_2 levels disappears for large ΔN , although, unlike the F_3 levels where we can see that the preference ends for $\Delta N \sim 4$ for He and Ar (and perhaps $\Delta N \sim 10$ for Xe), we cannot tell precisely where the decided preference for F_1 over F_2 ends. Alternatively, the appreciable F_2 level intensity may result from multiple-collision events.

We may interpolate and extrapolate our measured final-state specific cross-sections according to the trends expressed in Figs. 4 and 5, to all ΔN in order to estimate the size of the total cross-section for rotational transfer out of the initially pumped rotational level. The uncertainties for the individual cross-sections rapidly add up during this summation, resulting in a large relative uncertainty in the sum. Nevertheless, the results are consistent with the total cross-sections determined independently, by a different method, in I. The results are listed in Table 4. For helium and argon the summed results are somewhat larger than the directly measured values, although within the error limits. The directly measured values are certainly more precise than those given by this summing method. A better check of these total rotation cross-sections was performed by measuring areas within fluorescence bands rotationally relaxed by helium and argon collision partners under this higher resolution, which was the technique employed in I. Agreement within ten per cent for all gases is found using this method.

The conclusion in I, based on studies of band contours, that heavier collision partners induce larger rotational jumps in S_2^* than lighter ones is confirmed by the state-to-state cross-sections. Table 5 lists the F_1 state-to-state cross-sections for Table 3 as percentages of the total rotational transfer cross-sections from I. The results show that helium is more likely to cause smaller changes in the rotational motion of S_2^* than either argon or xenon as the result of a single rotation-changing collision.

ACKNOWLEDGMENTS

We thank the National Science Foundation for furnishing support for the portion of this project carried out while both authors were at the University of Wisconsin, and the E. I. DuPont de Nemours Company for providing summer research funds to one of us (TAC).

TABLE 4. TOTAL ROTATIONAL RELAXATION CROSS SECTIONS (\AA^2)

Gas	State-to-State Sum	Direct Measurement (Ref. 1)
He	50 ± 15	37 ± 4
Ar	80 ± 30	65 ± 7
Xe	70 ± 20	72 ± 7

TABLE 5. F₁ STATE-to-STATE RATES AS PERCENTAGES
OF THE TOTAL ROTATIONAL RELAXATION RATE

N'	He	Ar	Xe
50	2.9±0.9	2.9±1.4	2.7±0.8
46	5.5±1.3	4.6±1.7	3.3±0.8
44	7.1±2.1	5.6±2.1	3.8±1.2
42	15±3	14±3	8.0±1.6
38	13±2	11±3	8.6±1.8
36	6.9±1.4	5.8±1.5	4.0±1.2
34	5.2±1.0	4.1±1.1	3.7±0.7

REFERENCES

1. T. A. Caughey and D. R. Crosley, "Collision-Induced Energy Transfer in the $B^3\Sigma_u^-$ State of Diatomic Sulfur", J. Chem. Phys., 69, 3379-3396 (1978), referred to as I.
2. T. A. Caughey and D. R. Crosley, "Coherence Retention During Rotationally Inelastic Collisions of Selectively Excited Diatomic Sulfur", Chem. Phys. 20, 467-476, (1977).
3. K. A. Meyer and D. R. Crosley, "Rotational Satellite Intensities and Triplet Splitting in the $B^3\Sigma_u^-$ State of S_2 ", Can. J. Phys. 51, 2119-2121, (1973).
4. As is customary, $\Delta J \equiv J' - J''$ and $\Delta N \equiv N' - N''$ here.
5. S. M. Naude, "...Die Rotationsstruktur des Bandenspektrums des Schwefelmolekules S_2 ", Ann. Phys. (Leipzig) 3, 201-222, (1948).
6. R. F. Barrow and R. P. du Parc, in Elemental Sulfur, edited by B. Meyer (Interscience, New York, 1965), p. 251.
7. E. Olsson, "Das Bandenspektrum des Schwefels", Z. Phys. 100, 656-664 (1936).
8. T. A. Caughey, "Collisional Energy Transfer in B-State Diatomic Sulfur", PH. D. Thesis, University of Wisconsin, Madison, WI, (1977).
9. J. I. Steinfeld and W. Klemperer, "Energy Transfer in Monochromatically Excited Iodine Molecules", J. Chem. Phys. 42, 3475 (1965).
10. More precisely, the N, J level since both quantum numbers are actually necessary for a full description.
11. T. A. Caughey, K. A. Meyer and D. R. Crosley, "Lifetimes in the $B^3\Sigma_u^-$ State of S_2 ", to be published.
12. The cell temperature of 900 K is used to calculate the mean relative velocity.
13. M. Robinson and J. I. Steinfeld, "Entropy Analysis of Product Energy Distributions in Nonreactive Inelastic Collisions", Chem. Phys. 4, 467-475 (1974).
14. H. P. Broida and T. Carrington, "Rotational, Vibrational and Electronic Energy Transfer in the Fluorescence of Nitric Oxide", J. Chem. Phys. 38, 136-147 (1961).
15. R. K. Lengel and D. R. Crosley, "Energy Transfer in $A^2\Sigma^+ OH$. I. Rotational", J. Chem. Phys. 67, 2085-2101 (1977).

APPENDIX

We consider a calculation of the fraction $x(n)$ of excited S_2^* molecules which have undergone n rotation-state-changing collisions prior to radiating, under steady-state conditions. We begin with $m(n,t)$, the number of S_2^* molecules which have undergone n such collisions before radiation at a time t after excitation. This is given by the product of the probability $P(n,t)$ of undergoing n collisions in time t multiplied by $S^*(t)$, the total number of S_2^* molecules which have not already decayed by radiating, quenching, or vibrationally transferring.

$$m_n(t) = P(n,t) S^*(t).$$

$P(n,t)$ is given by a Poisson distribution:

$$P(n,t) = (R' A t / \tau)^n \exp(-R' A t / \tau) / n!.$$

Note that $(R' A / \tau)$ is independent of t since the collision dynamics are independent of how long the excited molecule has lived. Then S^* is given by:

$$S^* = S_0^* \exp[-(1 + Q_S' S + V' A) t / \tau].$$

To find x , we integrate $m(n,t)$ over all time, yielding

$$x = \frac{(1 + Q_S' S + V' A)}{(1 + Q_S' S + V' A + R' A)} \frac{R' A}{1 + Q_S' S + V' A + R' A}^n.$$

The fractions quoted in the main body of the text are calculated using rate constant values from Ref. 1.

DISTRIBUTION LIST

<u>No. of Copies</u>	<u>Organization</u>	<u>No. of Copies</u>	<u>Organization</u>
12	Commander Defense Technical Info Center ATTN: DDC-DDA Cameron Station Alexandria, VA 22314	1	Commander US Army Armament Materiel Readiness Command ATTN: DRSAR-LEP-L, Tech Lib Rock Island, IL 61299
1	Director Defense Advanced Research Projects Agency ATTN: LTC C. Buck 1400 Wilson Boulevard Arlington, VA 22209	1	Director US Army ARRADCOM Benet Weapons Laboratory ATTN: DRDAR-LCB-TL Watervliet, NY 12189
2	Director Institute for Defense Analysis ATTN: H. Wolfhard R. T. Oliver 400 Army-Navy Drive Arlington, VA 22202	1	Commander US Army Watervliet Arsenal ATTN: Code SARWV-RD, R.Thierry Watervliet, NY 12189
1	Commander US Army Materiel Development and Readiness Command ATTN: DRCDMD-ST 5001 Eisenhower Avenue Alexandria, VA 22333	1	Commander US Army Aviation Research and Development Command ATTN: DRSARV-E P. O. Box 209 St. Louis, MO 63166
2	Commander US Army Armament Research and Development Command ATTN: DRDAR-TSS Dover, NJ 07801	1	Director US Army Air Mobility Research and Development Laboratory Ames Research Center Moffett Field, CA 94035
5	Commander US Army Armament Research and Development Command ATTN: DRDAR-LCA, J. Lannon DRDAR-LC, T.Vladimiroff DRDAR-LCE, F. Owens DRDAR-SCA, L. Stiefel DRDAR-LC, D. Downs Dover, NJ 07801	1	Commander US Army Communications Rsch and Development Command ATTN: DRDCO-PPA-SA Fort Monmouth, NJ 07703
		1	Commander US Army Electronics Research and Development Command Technical Support Activity ATTN: DELSD-L Fort Monmouth, NJ 07703

DISTRIBUTION LIST

<u>No. of Copies</u>	<u>Organization</u>	<u>No. of Copies</u>	<u>Organization</u>
1	Commander US Army Missile Command ATTN: DRSMI-R Redstone Arsenal, AL 35809	1	Director US Army TRADOC Systems Analysis Activity ATTN: ATAA-SL, Tech Lib White Sands Missile Range NM 88002
1	Commander US Army Missile Command ATTN: DRSMI-YDL Redstone Arsenal, AL 35809	2	Office of Naval Research ATTN: Code 473 G. Neece 800 N. Quincy Street Arlington, VA 22217
1	Commander US Army Natick Research and Development Command ATTN: DRXRE, D. Sieling Natick, MA 01762	1	Commander Naval Sea Systems Command ATTN: J.W. Murrin, SEA-62R2 National Center Bldg. 2, Room 6E08 Washington, DC 20360
1	Commander US Army Tank Automotive Research & Development Cmd ATTN: DRDTA-UL Warren, MI 48090	1	Commander Naval Surface Weapons Center ATTN: Library Br., DX-21 Dahlgren, VA 22448
1	Commander US Army White Sands Missile Range ATTN: STEWS-VT White Sands, NM 88002	2	Commander Naval Surface Weapons Center ATTN: S. J. Jacobs, Code 240 Code 730 Silver Spring, MD 20910
1	Commander US Army Materials and Mechanics Research Center ATTN: DRXMR-ATL Watertown, MA 02172	1	Commander Naval Underwater Systems Cmd Energy Conversion Department ATTN: R.S. Lazar, Code 5B331 Newport, RI 02840
3	Commander US Army Research Office ATTN: Tech Lib D. Squire F. Schmiedeshaff R. Ghirardelli M. Ciftan P. O. Box 12211 Research Triangle Park NC 27706	2	Commander Naval Weapons Center ATTN: R. Derr C. Thelen China Lake, CA 93555

DISTRIBUTION LIST

<u>No. of Copies</u>	<u>Organization</u>	<u>No. of Copies</u>	<u>Organization</u>
1	Commander Naval Research Laboratory ATTN: Code 6180 Washington, DC 20375	1	Atlantic Research Corporation ATTN: M. K. King 5390 Cherokee Avenue Alexandria, VA 22314
3	Superintendent Naval Postgraduate School ATTN: Tech Lib D. Netzer A. Fuhs Monterey, CA 93940	1	AVCO Corporation AVCO Everett Research Lab Div ATTN: D. Stickler 2385 Revere Beach Parkway Everett, MA 02149
2	Commander Naval Ordnance Station ATTN: A. Roberts Tech Lib Indian Head, MD 20640	1	Foster Miller Associates, Inc. ATTN: A. J. Erickson 135 Second Avenue Waltham, MA 02154
3	AFOSR (B.T. Wolfson; D. Ball; L. Caveny) Bolling AFB, DC 20332	1	General Electric Company Armament Department ATTN: M. J. Bulman Lakeside Avenue Burlington, VT 05402
2	AFRPL (DYSC) ATTN: D. George J. N. Levine Edwards AFB, CA 93523	1	General Electric Company Flight Propulsion Division ATTN: Tech Lib Cincinnati, OH 45215
2	National Bureau of Standards ATTN: J. Hastie T. Kashiwagi Washington, DC 20234	2	Hercules Incorporated Alleghany Ballistic Lab ATTN: R. Miller Tech Lib Cumberland, MD 21501
1	Lockheed Palo Alto Rsch Labs ATTN: Tech Info Ctr 3521 Hanover Street Palo Alto, CA 94304	1	Hercules Incorporated Bacchus Works ATTN: B. Isom Magna, UT 84044
1	Aerojet Solid Propulsion Co. ATTN: P. Micheli Sacramento, CA 95813	1	IITRI ATTN: M. J. Klein 10 West 35th Street Chicago, IL 60615
1	ARO Incorporated ATTN: N. Dougherty Arnold AFS, TN 37389		

DISTRIBUTION LIST

<u>No. of</u> <u>Copies</u>	<u>Organization</u>	<u>No. of</u> <u>Copies</u>	<u>Organization</u>
1	Olin Corporation Badger Army Ammunition Plant ATTN: J. Ramnarace Baraboo, WI 53913	1	Shock Hydrodynamics, Inc. ATTN: W. H. Anderson 4710-16 Vineland Avenue North Hollywood, CA 91602
2	Olin Corporation New Haven Plant ATTN: R.L. Cook D.W. Riefler 275 Winchester Avenue New Haven, CT 06504	1	Thiokol Corporation Elkton Division ATTN: E. Sutton Elkton, MD 21921
1	Paul Gough Associates, Inc. ATTN: P.S. Gough P. O. Box 1614 Portsmouth, NH 03801	3	Thiokol Corporation Huntsville Division ATTN: D. Flanigan R. Glick Tech Lib Huntsville, AL 35807
1	Physics International Co. 2700 Merced Street Leandro, CA 94577	2	Thiokol Corporation Wasatch Division ATTN: J. Peterson Tech Lib P. O. Box 524 Brigham City, UT 84302
1	Pulsepower Systems, Inc. ATTN: L. C. Elmore 815 American Street San Carlos, CA 94070	1	TRW Systems Group ATTN: H. Korman One Space Park Redondo Beach, CA 90278
3	Rockwell International Corp. Rocketdyne Division ATTN: C. Obert J. E. Flanagan A. Axeworthy 6633 Canoga Avenue Canoga Park, CA 91304	2	United Technology Center ATTN: R. Brown Tech Lib P. O. Box 358 Sunnyvale, CA 94088
2	Rockwell International Corp. Rocketdyne Division ATTN: W. Haymes Tech Lib McGregor, TX 76657	1	Universal Propulsion Co. ATTN: H.J. McSpadden 1800 W. Deer Valley Road Phoenix, AZ 85027
1	Science Applications, Inc. ATTN: R. B. Edelman Combustion Dynamics and Propulsion Division 23146 Cumorah Crest Woodland Hills, CA 91364	11	Battelle Memorial Institute ATTN: Tech Lib R. Bartlett (10 cys) 505 King Avenue Columbus, OH 43201

DISTRIBUTION LIST

<u>No. of Copies</u>	<u>Organization</u>	<u>No. of Copies</u>	<u>Organization</u>
1	Brigham Young University Dept of Chemical Engineering ATTN: M. W. Beckstead Provo, UT 84601	1	Pennsylvania State University Dept of Mechanical Engineering ATTN: K. Kuo University Park, PA 16801
1	California Institute of Tech 204 Karmar Lab Mail Stop 301-46 ATTN: F.E.C. Culick 1201 E. California Street Pasadena, CA 91125	1	Pennsylvania State University Dept of Material Sciences ATTN: H. Palmer University Park, PA 16801
1	Case Western Reserve Univ. Division of Aerospace Sciences ATTN: J. Tien Cleveland, OH 44135	2	Princeton University Forrestal Campus ATTN: I. Glassman Tech Lib P. O. Box 710 Princeton, NJ 08540
3	Georgia Institute of Tech School of Aerospace Eng. ATTN: B. T. Zinn E. Price W.C. Strahle Atlanta, GA 30332	2	Purdue University School of Mechanical Eng ATTN: J. Osborn S.N.B. Murthy TSPC Chaffee Hall West Lafayette, IN 47906
1	Institute of Gas Technology ATTN: D. Gidaspo 3424 S. State Street Chicago, IL 60616	1	Rutgers State University Dept of Mechanical and Aerospace Engineering ATTN: S. Temkin University Heights Campus New Brunswick, NJ 08903
1	Johns Hopkins University/APL Chemical Propulsion Info Agency ATTN: T. Christian Johns Hopkins Road Laurel, MD 20810	4	SRI International ATTN: Tech Lib D. Crosley J. Barker D. Golden 333 Ravenswood Avenue Menlo Park, CA 94025
1	Massachusetts Inst of Tech Dept of Mechanical Engineering ATTN: T. Toong Cambridge, MA 02139	1	Stevens Institute of Tech Davidson Library ATTN: R. McAlevy, III Hoboken, NJ 07030
1	Pennsylvania State University Applied Research Lab ATTN: G. M. Faeth P. O. Box 30 State College, PA 16801		

DISTRIBUTION LIST

<u>No. of Copies</u>	<u>Organization</u>
1	University of California, San Diego Ames Department ATTN: F. Williams P. O. Box 109 La Jolla, CA 92037
1	University of Illinois Dept of Aeronautical Eng ATTN: H. Krier Transportation Bldg, Rm 105 Urbana, IL 61801
1	University of Minnesota Dept of Mechanical Eng. ATTN: E. Fletcher Minneapolis, MN 55455
1	University of Southern California Department of Chemistry ATTN: S. Benson Los Angeles, CA 90007
1	University of Texas Dept of Chemistry ATTN: W. Gardiner H. Schaefer Austin, TX 78712
2	University of Utah Dept of Chemical Engineering ATTN: A. Baer G. Flandro Salt Lake City, UT 84112
<u>Aberdeen Proving Ground</u>	
	Dir, USAMSAA ATTN: DRXSY-D DRXSY-MP, H. Cohen Cdr, USATECOM ATTN: DRSTE-TO-F Dir, USA CSL, Bldg. E3516 ATTN: DRDAR-CLB-PA

USER EVALUATION OF REPORT

Please take a few minutes to answer the questions below; tear out this sheet and return it to Director, US Army Ballistic Research Laboratory, ARRADCOM, ATTN: DRDAR-TSB, Aberdeen Proving Ground, Maryland 21005. Your comments will provide us with information for improving future reports.

1. BRL Report Number _____

2. Does this report satisfy a need? (Comment on purpose, related project, or other area of interest for which report will be used.)

3. How, specifically, is the report being used? (Information source, design data or procedure, management procedure, source of ideas, etc.)

4. Has the information in this report led to any quantitative savings as far as man-hours/contract dollars saved, operating costs avoided, efficiencies achieved, etc.? If so, please elaborate.

5. General Comments (Indicate what you think should be changed to make this report and future reports of this type more responsive to your needs, more usable, improve readability, etc.)

6. If you would like to be contacted by the personnel who prepared this report to raise specific questions or discuss the topic, please fill in the following information.

Name: _____

Telephone Number: _____

Organization Address: _____

